33RD INTERNATIONAL COSMIC RAY CONFERENCE, RIO DE JANEIRO 2013
THE ASTROPARTICLE PHYSICS CONFERENCE

ICRC 2013

The Viability of Low-Mass Subhalos as Targets for Gamma-Ray Dark Matter Searches

ANDREA KLEIN[1,2], MIGUEL A. SÁNCHEZ-CONDE[1,3]

[1] *Stanford University, Stanford, CA 94305, USA*
[2] *Carnegie Mellon University, Pittsburgh, PA 15213, USA*
[3] *SLAC National Accelerator Laboratory & Kavli Intitute for Particle Astrophysics and Cosmology, 2575 Sand Hill Road, Menlo Park, CA 94025, USA*

alklein@alumni.stanford.edu

Abstract: In the concordance cosmological model, cold dark matter (DM) halos exhibit significant substructure, including many gravitationally-bound subhalos. If DM is made of Weakly Interacting Massive Particles that self-annihilate into standard particles, nearby subhalos might be among the best astrophysical candidates for indirect DM detection by the Fermi Large Area Telescope and current Cherenkov telescopes. Past efforts to compute the expected number of potentially detectable subhalos have concentrated on the prospects of detecting very high-mass subhalos. Using the highest-resolution DM simulations available, namely Via Lactea II and Aquarius, we instead make detectability predictions for low-mass subhalos. Since both simulations offer an incomplete representation of subhalos lighter than about a million solar masses, we extrapolate the subhalo properties found above the mass resolution limits in the simulations. This allows us to selectively repopulate the original simulations with the brightest low-mass subhalos, including the first such results for objects lighter than one solar mass. We also study the impact of different methodological approaches, including the use of several different models that describe internal subhalo structure, on the final results. Finally, we apply bootstrapping techniques in order to quantify the statistical uncertainties. Our results suggest that low-mass subhalos should not be neglected as candidates for γ-ray DM searches, as some of them could exhibit DM annihilation fluxes comparable to that of the Draco dwarf galaxy.

Keywords: dark matter galaxies: dwarf gamma rays: galaxies methods: numerical.

1 Introduction

In the current standard model of cosmology (ΛCDM), small dark matter (DM) structures form first and later merge to form larger structures. This hierarchical structure formation scenario predicts that gravitationally-bound structures, known as halos, that host galaxies like our own are abundantly populated with bound substructures, or subhalos. Current cosmological N-body simulations of Milky Way-sized halos [1, 2] predict the existence of thousands of galactic subhalos with masses $> 10^6\ M_\odot$ and many more with smaller masses. The most massive of these are believed to host the observed Milky Way satellite galaxies, while those with smaller masses may host no stars or gas and would thus be completely dark satellites, i.e. weak γ-ray sources with no astrophysical counterparts at other wavelengths. Given their distances and masses, these small DM subhalos may be among the best candidates for γ-ray DM searches [3].

The Large Area Telescope (LAT) aboard the Fermi Gamma Ray Space Telescope continually surveys the entire γ-ray sky with unprecedented sensitivity, making it an ideal instrument for the discovery of new source classes. In particular, the LAT has the potential to detect γ-ray signals from WIMP annihilation within DM subhalos. Previous estimates predict that $0.1 - 100$ subhalos may be detectable by the LAT, depending on the assumed DM particle properties and simulation parameters [4, 5]. These studies have largely concentrated on the viability of the most massive subhalos as indirect detection targets. However, a detailed understanding of the whole DM subhalo population is essential to planning the best DM search strategy, by the LAT and by future instruments. It is also critical if we are to identify potential subhalo candidates from among the 576 unidentified γ-ray sources in the 2FGL Fermi catalog [6].

The Aquarius (AQA) [1] and Via Lactea II (VL-II) [2] N-body cosmological simulations provide the highest-resolution galactic-scale simulations available. Yet, these simulations fail to resolve the subhalo hierarchy below a mass of $\sim 10^5$ $M_\odot$. In comparison, the theoretical minumum subhalo mass may be as low as 10^{-6} $M_\odot$ [7]. Consequently, these simulations offer incomplete data for the purposes of low-mass subhalo detection studies.

In this work, we will make use of well motivated semi-analytical extrapolations to assess the contribution of nearby, low-mass subhalos to the total population of potentially detectable subhalos. Taking into account both our knowledge of the parent simulations and the expected internal properties of low-mass subhalos in the standard cosmology, we implement several key refinements to previous efforts in this direction. Using these extrapolations, we will supplement the AQA and VL-II subhalo datasets with subhalos less massive than their resolution limits. We will also resample the complete subhalo populations in order to extract statistically meaningful predictions and quantify the corresponding uncertainties. We will present the first such results for subhalos as light as $10^{-2}\ M_\odot$, many orders of magnitude below the resolution limits of the original simulations. By using independently generated simulations, we hope to derive more robust results, as well as to identify any noteworthy disagreements in their predictions. Some difference is expected in any case, since e.g. each simulation assumes different cosmological parameters, namely those of WMAP3 (AQA) and WMAP5 (VL-II).

These proceedings are organized as follows: Section 2 provides an overview of our methodology, with particular emphasis on the semi-analytical models that underlie our extrapolations. Section 3 presents our primary results, including some discussion of the relative impact of different methodological choices on the final outcome of halo repopulation. We also include some final commentary and conclusions, including a brief discussion of our results in the context of the ongoing DM search effort by the LAT. Under the most physically realistic assumptions, we consistently find that a significant number of low-mass DM subhalos exhibit annihilation fluxes competitive with those of the higher-mass subhalos currently regarded to be viable search targets.

2 Methodology

The aim of halo repopulation is to produce a dataset in the style of the original AQA and VL-II simulations, with some key differences. Namely, we adopt simulation-specific mass cuts, and we generate all lighter subhalos via our semi-analytic extrapolations. The resulting "repopulated" halos are no longer underpopulated at low mass, and subhalos much lighter than the original resolution limits are included. We achieve this in a relatively efficient manner by drawing the masses and distances of the new subhalos from probability density functions, with some additional physics imposed. Next we characterize the internal subhalo properties by assigning to each subhalo a *concentration* depending only on its total mass. A subhalo's concentration will in turn specify its DM annihilation luminosity, a key metric of detectability.

Once we have generated a dataset in this manner for each parent simulation, we resample it many times. This permits us to learn the average and variance in the number of detectable subhalos as a function of the parent halo and the concentration model used during the dataset's creation. Below, we present the complete recipe for repopulating and resampling a simulation dataset.

2.1 Subhalo mass and radial distributions

In order to generate all properties of interest for low-mass subhalos, we adopt semi-analytical models of the parent halos' mass and radial distribution functions. Following Ref. [5], we decompose the total DM density profile of the parent halo, $\rho_{total}(r)$, into the sum of a smooth component $\rho_{smooth}(r)$ plus a component $\rho_{sub}(r)$ that accounts for the resolved subhalos. VL-II's total density profile can be fit to a Navarro-Frenk-White (NFW) profile [2], whereas AQA is better modeled by an Einasto profile [1]:

$$\rho_{total}^{VL-II}(r) = \frac{4\rho_s}{\frac{r}{r_s}\left(1+\frac{r}{r_s}\right)^2} \tag{1}$$

$$\rho_{total}^{AQ}(r) = \rho_s \exp\left\{-\frac{2}{\alpha}\left[\frac{r}{r_s}^{\alpha} - 1\right]\right\} \tag{2}$$

Here, r is the distance to the Galactic Center (GC), and ρ_s and r_s are the best-fit scale density and scale radius, respectively, of the parent simulation.

The simulations also differ in their predictions for the subhalo radial distributions inside the host halo. ρ_{sub}^{VL-II} follows a distribution antibiased to ρ_{total}^{VL-II}, whereas ρ_{sub}^{AQ} has the same shape as ρ_{total}^{AQ}. Both simulations have a subhalo mass function of the form $\rho \propto \left(\frac{M_{sub}}{M_\odot}\right)^{-\mu}$ differing only in the value of μ, which is 1.9 for AQA and 2.0 for VL-II.

2.2 Subhalo Internal Structure

We will use concentration as the key parameter to model the internal structure of subhalos, which ultimately has a critical impact on subhalo detectability. The halo concentration is formally defined as the ratio between the halo radius and its scale radius. We will consider several different models for the subhalo concentration-mass relation, $c(M)$. We will adopt, for each simulation, an intentional overestimate $c_{max}(M)$, a physically-motivated intermediate model $c_{med}(M)$, and an intentional underestimate $c_{min}(M)$. Each simulation's overestimate $c_{max}(M)$ is taken from power-law fit to the concentrations above the mass cuts. The underestimate $c_{min}(M)$ is simply a constant set to the value of $c_{max}(M)$ and $c_{med}(M)$ at the mass cut M_{cut}, where we require that $c_{max}(M_{cut}) = c_{med}(M_{cut})$.

It is important to keep in mind that $c_{max}(M)$ and $c_{min}(M)$ are not realistic, since they deviate significantly from physically-motivated $c(M)$ models ([8, 9]). Nonetheless, for the purposes of this work, we believe that it is useful to include results for both kinds of unrealistic concentration models, as they perfectly illustrate the importance of using a more sophisticated $c(M)$ model in low-mass subhalo detectability studies. Note that some of the previous low-mass extrapolations performed in the literature implicitly assumed one of these unrealistic models (e.g. [10]).

We follow Ref. [12] to set c_{med}^{AQ}. This $c(M)$ model is based on previous work by Bullock et al. [8] and adopts the functional form proposed in [13] with slightly different parameters:

$$\ln(c_{med}^{AQ}) = \sum_{i=0}^{4} c_i^{FHM} \times \left[\ln\left(\frac{M}{M_\odot}\right)\right]^i \tag{3}$$

where $c^{FHM} = [4.265, -0.0384, -3.91\cdot10^{-4}, -2.2\cdot10^{-6}, -5.5\cdot10^{-7}]$. c_{med}^{VL} is the best fit to the original simulation above the mass cut as given in [5]:

$$c_{med}^{VL} = \left[C_1\left[\frac{M_{sub}}{M_\odot}\right]^{\alpha_1} + C_2\left[\frac{M_{sub}}{M_\odot}\right]^{\alpha_2}\right] \tag{4}$$

where $(C1, C2) = (119.75, -85.16)$ and $(\alpha_1, \alpha_2) = (-0.012, -0.0026)$.

We schematically summarize the relationship between the VL-II $c(M)$ models in Fig. 1. The AQA models bear a similar relationship to one another; note, however, that AQA predicts somewhat higher concentrations overall than VL-II.

In each simulation, we also compensate for the higher concentration of subhalos relative to field halos (see e.g. [14]) by converting the halo concentrations given by the $c(M)$ models above to subhalo concentrations, $c_{sub}(M,R)$:

$$c_{sub}(M,R) = c_{vir}(M)\left(\frac{R}{R_{vir}^{host}}\right)^{-\alpha_D} \tag{5}$$

where R is the distance to the GC and R_{vir}^{host} is the virial radius of the host halo, 433 and 402 kpc for AQA and VL-II, respectively. The power-law slope $\alpha_D = 0.237$ for AQA and 0.286 for VL-II.

Finally, we also include an intrinsic scatter about the mean value $\bar{c}$ given by $c_{sub}(M,R)$ to account for the stochastic nature of halo formation. The corresponding probability

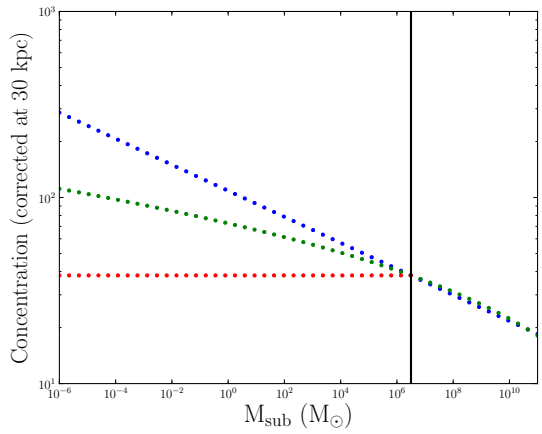

Fig. 1: VL-II concentration models assumed in this work below the mass cut of the parent simulation (vertical line). In this example, concentrations were corrected by applying eq. (5) at 30 kpc from the Galactic Center. See text for details.

follows a log-Gaussian distribution (see e.g. [12]), where we adopt $\sigma_{\log_{10} c} = 0.14$ following previous work [8, 15].

2.3 Relative Detectability Calculation

The total gamma-ray flux ϕ due to WIMP annihilation within a subhalo is given by the product of the so-called astrophysical J-factor $J(\psi)$ and a component Φ^{PP} which depends on the particular choice of particle physics model for WIMP annihilation:

$$\phi(E,\psi) = J(\psi) \times \Phi^{PP}(E) \tag{6}$$

The astrophysical J-factor is equal to the line-of-sight (l.o.s.) integral of the square of the DM density, $\rho(r)$, integrated over the solid angle subtended by the subhalo:

$$J(\psi) = \int_{l.o.s.} \rho(l(\psi))^2 dl \tag{7}$$

where the angle ψ represents the angle between the center of the subhalo and the l.o.s. Of the known satellite galaxies, the Draco dwarf galaxy has one of the highest J-factors, roughly $2 \cdot 10^{12}\ M_\odot/kpc^5$, and thus is expected to produce a high gamma-ray flux relative to many other dwarfs, e.g. [16]. In the following, we will take Draco's J-factor as our reference J-factor value. As for the parameter Φ^{PP}, although it is unknown, it should be the same for Draco as for any other DM satellites. The J-factor can therefore be used directly as a metric of relative detectability, without invoking any assumptions about the details of WIMP annihilation. In this study, we will only consider subhalos with J-factors down to a tenth of Draco's, i.e. $2 \cdot 10^{11}\ M_\odot/kpc^5$, following [3].

For convenience, instead of dealing directly with the J-factors as defined above, we have expressed our result in terms of J-factors relative to the J-factor of Draco, J_D. Assuming the mass distribution within each subhalo follows an NFW profile, we can compute the J-factor, relative to J_D, of each subhalo. A subhalo will be more luminous than $R \times J_D$ provided that $J_R = \frac{J_{sub}}{J_D} \geq R$, where J_R is given by

$$J_R = \left(\frac{D_D}{D_{sub}}\right)^2 \left(\frac{M_{sub}}{M_D}\right) \left(\frac{c_{sub}}{c_D}\right)^3 \left(\frac{f(c_D)}{f(c_{sub})}\right)^2 \tag{8}$$

where $f(c) = \ln(1+c) - c/(1+c)$. For each concentration model, we calculate c_D using the $c(M)$ relations given in Section 2.4 assuming $8 \cdot 10^8 M_\odot$ for the mass of Draco [16]. We take $D_D = 80$ kpc [17]. Note that in eq. (8) above, the distances D_{sub} and D_D to the subhalo and Draco, respectively, are relative to the Earth, rather than to the GC.

2.4 Radial Cuts

We adopt two interrelated criteria by which we exclude subhalos from certain radial ranges. The first is the Roche criterium, which accounts for tidal disruption: a subhalo can be considered totally disrupted by tidal forces when its tidal radius R_{tidal} exceeds its scale radius, r_s. We define the Roche cut, $R_{roche}(M)$, as the radius at which $R_{tidal}(M)$ and $r_s(M)$ intersect, i.e. the minimum galactocentric radius at which a subhalo of mass M can reside.

We also introduce a conservative radial detectability cut to reduce the number of unnecessary subhalos, from the point of view of our study, generated in a given mass range. We reject subhalos with J-factors smaller than R times Draco's J-factor by cutting at

$$R_{cut}(M) \approx \sqrt{\frac{M\, D_D^2\, c(M)^3\, f(c_D)^2}{R\, f(c)^2\, M_D\, c_D^3}} \tag{9}$$

relative to the GC, with $R = 0.1$. In this equation, $c(M)$ is the one given by eq. (5) at R_{Roche}. In this way, we are conservative in estimating R_{cut}.

When we impose radial cuts, we repopulate shells centered on the GC, rather than the Earth, because retaining this spherical symmetry makes the data more amenable to resampling. Thus we greatly reduce the number of generated subhalos, which speeds up the code, but we retain the option to apply the boostrapping method described in the next section to our output files.

2.5 Bootstrapping

Ultimately, for each concentration model, we produce one repopulated dataset for each of AQA and VL-II in the style of the original simulations, i.e. an array of subhalos, where each 'subhalo' is a vector of parameter values (mass, position, distance from Earth, relative J-factor). We then derive statistics from the repopulated files via bootstrapping. Bootstrapping simply refers to randomized sampling with replacement, where in this context the randomization is over the subhalos in a simulation dataset. Bootstrapping a subhalo dataset makes it possible to rapidly generate thousands of datasets resembling but not identical to the original. The variation in the number of detectable subhalos amongst the bootstrapped files provides an estimate of the variation one might expect in a population of many fully rendered galactic simulations.

The simple bootstrap procedure just described preserves the individual subhalos intact. Hence, all of the detectable subhalos in a bootstrapped simulation will be subhalos that were considered detectable in the original data. Furthermore, nothing prevents the same subhalo from appearing more than once in a given bootstrapped file. We also find that the same few subhalos show up as detectable in the majority of the bootstrapped files when this method is used. In an effort to compensate for these effects and keep the bootstrapped datasets as statistically independent as possible, in addition to selecting subhalos randomly from the parent distribution, we have spatially "reshuffled" the subhalos randomly. That is, we move each subhalo to a uniformly random location on

the sphere defined by its radial position relative to the halo center prior to resampling. We then recalculate its relative J-factor at its new radial position.

This method of reshuffling maintains each subhalo at a radial position consistent with its mass and thus preserves the radial mass distribution of the parent simulation. Similarly, the subhalos' concentrations, and therefore their annihilation luminosities, are unaffected. However, reshuffled bootstrapping brings different subhalos within a detectable distance of the Earth in different realizations, so the bootstrapped files are less dependent on the original file.

3 Results

We have generated repopulated datasets from $10^{-2}M_{\odot}$ to the maximum subhalo mass of each original simulation; we then resampled each repopulated file via reshuffled bootstrapping 100 times. We find that VL-II predicts a somewhat higher number of potentially detectable subhalos overall. For example, on average, the repopulated VL-II $c_{med}(M)$ gives 1114 subhalos with $J_R > 0.1$, whereas AQA gives an average of 650. Likewise there is some difference in the standard deviations: 24 for VL-II and 14 for AQA.

As expected, for both simulations, c_{max} and c_{min} provide much looser bounds on the expected number of luminous subhalos. For example, for VL-II, c_{max} predicts an average of 1812 subhalos with $J_R > 0.1$, whereas c_{min} predicts an average of only 641. These values both lie well outside the range about VL-II's c_{med} average implied by the corresponding standard deviation. In other words, the c_{med} results deviate substantially from the results obtained by using either power-law extrapolation.

If we examine the subhalo populations in more detail, we find that while the majority of the very luminous subhalos have high mass, the contribution from the low-mass subhalos is not negligible. Indeed, the top panel in Fig. 2, which shows results from a typical run of the repopulation algorithm, includes several low-mass subhalos with J_R's in the range of $0.1-1$, and even a few with $J_R > 1$. This is because they lie relatively close to the Earth: as close as 10^{-2} kpc, as shown in the bottom panel of Fig. 2. Note that the mass range from $10^4-10^5 M_{\odot}$ hosts the majority of the potentially detectable subhalos, illustrating the importance of studying subhalos in this range carefully.

For purposes of detection with the Fermi-LAT, the spatial extension of the most luminous subhalos is also of particular interest. Any subhalos that exhibit significant spatial extension will be easier to distinguish from pointlike sources, such as pulsars, which might otherwise be confused for DM candidates. We find that most of the brightest subhalos are pointlike, although a few do have significant spatial extension, i.e. greater than a few degrees. Likewise, it is clear that the lightest subhalos, i.e. those most relevant to this study, are mostly pointlike.

In conclusion, we find that low-mass subhalos are expected to contribute importantly to the total population of potentially detectable subhalos. Indeed, a good number of them should possess DM annihilation fluxes comparable to that of the Draco dwarf galaxy, one of the most promising targets, or even substantially higher. In an upcoming paper, we will also provide repopulated subhalo datasets to aid in the study of these objects [18]. For instance, these datasets could be especially useful for inspecting unidentified γ-ray sources in the context of DM annihilation.

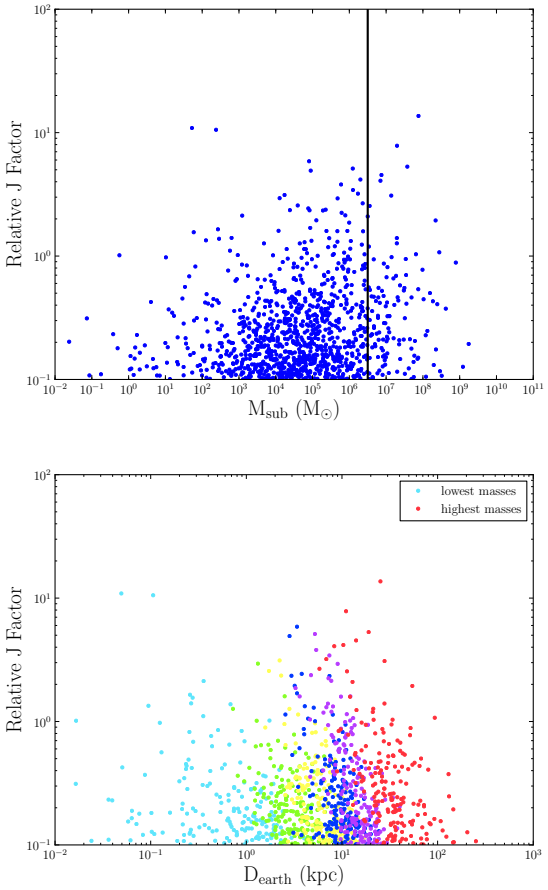

Fig. 2: VL-II J-factors vs. subhalo mass (top panel) and vs. subhalo distance from Earth (bottom panel) for the most luminous subhalos ($J_R > 0.1$). The J-factors are relative to Draco's. The vertical line corresponds to the mass cut we assumed for VL-II.

References

[1] V. Springel, et al., MNRAS 398 (2008) 1685
[2] J. Diemand, M. Kuhlen, and P. Madau, ApJ 657 (2007) 262
[3] M. Ackermann, et al., ApJ 747 (2012) 121
[4] B. Anderson, et al., ApJ 718 (2010) 899
[5] L. Pieri, et al., PRD 83 (2011) 023518
[6] P. Nolan, et al., ApJS 199 (2012) 31
[7] S. Profumo, et al., PRL 97 (2006) 031301
[8] J. Bullock et al., MNRAS 321 (2001) 559
[9] M. A. Sánchez-Conde and F. Prada (2013) in prep.
[10] A. Pinzke, et al., PRD 84 (2011) 123509
[11] L. Gao, et al., MNRAS 419 (2011) 1721
[12] H. Zechlin, et al., A&A 538 (2012) A93
[13] J. Lavalle, et al., A&A 479 (2008) 427
[14] J. Diemand, et al., Nature 454 (2008) 735
[15] R. Wechsler, et al., ApJ 568 (2002) 52
[16] M. A. Sánchez-Conde, et al., JCAP 12 (2011) 011
[17] A. Aparicio, R. Carrera and D. Martinez-Delgado, AJ 122 (2001) 2524
[18] A. Klein, M. A. Sánchez-Conde, A. Drlica-Wagner, E. Bloom (2013) in prep.